Acta Crystallographica Section B
Structural Science
ISSN 0108-7681

A variable-temperature study of a phase transition in barbituric acid dihydrate

Gary S. Nichol and William Clegg*

School of Natural Sciences – Chemistry, Bedson Building, University of Newcastle upon Tyne, Newcastle upon Tyne NE1 7RU, England

Correspondence e-mail: w.clegg@ncl.ac.uk

Received 5 March 2005
Accepted 31 May 2005

The crystal structure of barbituric acid dihydrate ($C_4H_4N_2O_3{\cdot}2H_2O$) has twice been reported as orthorhombic, space group *Pnma*, with all atoms (except for CH_2 H atoms) lying on the mirror plane [Al-Karaghouli *et al.* (1977). *Acta Cryst*. B**33**, 1655–1660; Jeffrey *et al.* (1961). *Acta Cryst*. **14**, 881–887]. The present study has found that at low temperatures, below 200 K, the crystal structure is no longer orthorhombic but is non-merohedrally twinned monoclinic, space group $P2_1/n$. This phase is stable down to 100 K. Above 220 K the crystal structure is orthorhombic, and between 200 and 220 K the structure undergoes a phase change, with the monoclinic-to-orthorhombic phase transition itself taking place at around 216–217 K. The size of the β angle in the monoclinic structure is temperature dependent; at 100 K β is around 94° and it decreases in magnitude towards 90° as the temperature increases. Although the hydrogen-bonding motifs are the same for both crystal systems, there are significant differences in the crystal packing, in particular the out-of-plane displacement of the two water molecules and the sp^3-hybridized C atom of barbituric acid.

1. Introduction

Over the past few years, the topic of phase transitions has become more and more popular for scientific investigation. This extremely broad field is actively pursued by physicists, chemists, materials scientists, earth scientists and metallurgists (Pandey, 2005). Indeed, the January 2005 edition of *Acta Crystallographica Section A: Foundations of Crystallography* was devoted almost entirely to the topic. A simple search in February 2005 of SciFinder Scholar 2004 (American Chemical Society, 2004) for 'phase transition' resulted in almost 138 500 hits; the top five years according to the greatest numbers of hits were 2003, 2002, 2001, 2000 and 2004. The number of hits in 2003 is 9013, more than double that of 1995 (4457) and a clear indication of the increasing interest in the subject.

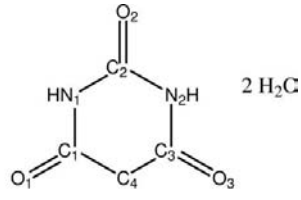

Barbituric acid dihydrate (I)
with atomic numbering scheme

Our interest in the temperature-induced phase transition of barbituric acid dihydrate arose from our research on metal complexes of this and related ligands. Barbituric acid is the

parent molecule of the barbiturate family of drugs, which are of crystallographic interest not least for their propensity to form polymorphs. The 5,5-dialkyl derivatives are those which are pharmacologically active and which have been most extensively characterized by X-ray crystallography (Caillet & Claverie, 1980; Cleverley & Williams, 1959; Craven *et al.*, 1969, 1982; Craven & Vizzini, 1969, 1971; McMullan *et al.*, 1978; Nichol & Clegg, 2005*a*,*b*; Platteau *et al.*, 2005; Sambyal *et al.*, 1995; Williams, 1973, 1974). Contemporary research continues to focus on barbituric acid polymorphism as a model system for developing computational polymorph prediction techniques, something that is of major importance to the pharmaceutical industry (Lewis *et al.*, 2004, 2005).

1.1. Analysis of current literature

The structure of barbituric acid dihydrate (I) appears twice in the primary literature: an X-ray diffraction study (Jeffrey *et al.*, 1961) and a neutron diffraction study (Al-Karaghouli *et al.*, 1977). In both reports the data collections were carried out at room temperature, and the crystal system and space group are reported as orthorhombic, *Pnma*. The final *R* factors are 0.14 and 0.087, respectively. Both reports conclude that, with the exception of the two H atoms of the CH_2 group, all atoms of the barbituric acid and water molecules lie on the mirror plane. During their discussions, both reports make mention of the high atomic displacement observed in the *b*-axis direction (*i.e.* perpendicular to the mirror plane). Al-Karaghouli *et al.* (1977) considered the possibility of an alternative non-centrosymmetric space group, $Pn2_1a$ (non-standard setting of $Pna2_1$), which would allow the atoms to deviate from the (now non-crystallographic) mirror plane. These authors also considered a model in which one of the O atoms was deliberately displaced off the mirror plane and then refined as disordered. Neither of these models gave a satisfactory outcome and they concluded that there was no good reason to doubt the assignment of *Pnma* as the space group.

2. Experimental

2.1. Preliminary experiments

With these uncertainties in mind, we carried out a low-temperature redetermination of barbituric acid dihydrate for the purpose of having a reference structure of the ligand for reliable comparison with the structures of our metal complexes, also determined routinely at low temperature. It was found that, at 150 K, the crystal system was not orthorhombic but non-merohedrally twinned monoclinic and the space group was $P2_1/n$. Curious to know whether this result pointed to inaccuracies in the literature reports (which were at least 27 years old), we re-collected data, from the same crystal, at room temperature. As reported by Jeffrey *et al.* (1961), the crystal decomposed on the diffractometer during data collection from a transparent colourless crystal to a white opaque solid, which did not diffract at all. Nevertheless, sufficient data were collected to confirm that at room temperature the structure is indeed orthorhombic with the space group *Pnma*. Hence the crystal had undergone a phase transition on warming from low temperature to room temperature (and, presumably, in the reverse direction in the initial flash-cooling). A variable-temperature X-ray diffraction study was carried out to observe the effect of changing temperature on the crystal structure and to determine at what point the phase transition occurs.

2.2. Sample preparation

Crystals of barbituric acid dihydrate were prepared by dissolving a sample of commercially available barbituric acid (obtained as a white powder from Lancaster Synthesis) in distilled water with gentle heating. Storage at 278 K over a weekend resulted in large colourless and perfectly transparent block crystals of barbituric acid dihydrate.

2.3. Experimental strategy

Data were collected on a Bruker SMART 1K CCD diffractometer fitted with an Oxford Cryosystems Cryostream cooler (Cosier & Glazer, 1986) at 14 different temperatures ranging from 100 to 270 K. Experimental details for selected temperatures are summarized in Table 1 (details for all experiments are available in the deposited supplementary material[1]). A large good-quality crystal, which did not require cutting, was selected from the sample and, on the basis of preliminary experiments, the experimental strategy was started by re-collecting data at 150 K and then proceeding in the following temperature order: 170, 190, 200, 210, 220, 230, 215, 217, 218, 219, 216, 100 and 270 K. A full data collection, as opposed to a simple unit-cell determination, was carried out at each temperature. Such a procedure adds several days to the time taken to conduct the experiments; however, it also allows for complete structure solution and refinement – the ultimate indicator of crystal system correctness and data quality – at each temperature and is especially important when one considers that the crystals were twinned in the monoclinic crystal system; a full data collection allows the determination of unit-cell parameters for both components of the twin from several hundred reflections, rather than the hundred or so that would be measured by only collecting partial data for an orientation matrix. The same data collection strategy (complete sphere of reciprocal space, 0.3° width frames, 30 s exposures) was used for each experiment.

The reasons for selecting two extreme temperatures to finish the strategy were to check that the crystal did not undergo a second phase transition at even lower temperatures; so we could verify that the phase transition is reversible; so that we could see that the crystal did not suffer physical stress at extreme cold; and so we could collect data as close to room temperature as possible without the crystal decomposing. The same crystal, pictured in Fig. 1, was used for every experiment;

[1] Supplementary data for this paper are available from the IUCr electronic archives (Reference: WS5026). Services for accessing these data are described at the back of the journal.

Table 1
Experimental details at selected temperatures.

Details for all experiments are given in the deposited CIF.

	100 K	200 K	215 K	217 K	230 K	270 K
Cell setting, space group	Monoclinic, $P2_1/n$	Monoclinic, $P2_1/n$	Monoclinic, $P2_1/n$	Orthorhombic, *Pmnb*	Orthorhombic, *Pmnb*	Orthorhombic, *Pmnb*
a, b, c (Å)	6.0970 (5), 12.7152 (10), 8.8587 (7)	6.1313 (12), 12.703 (2), 8.8456 (17)	6.1580 (9), 12.7515 (18), 8.8763 (13)	6.1770 (18), 12.785 (4), 8.898 (3)	6.1739 (4), 12.7594 (9), 8.8831 (6)	6.2144 (7), 12.7512 (14), 8.8841 (10)
β (°)	94.0510 (14)	92.187 (4)	91.263 (3)	90	90	90
V (Å^3)	685.05 (9)	688.5 (2)	696.83 (17)	702.7 (3)	699.77 (8)	703.99 (14)
D_x (Mg m^{-3})	1.591	1.583	1.564	1.551	1.558	1.549
No. of reflections for cell parameters	3196	4075	3413	4044	4267	3968
θ range (°)	2.3–28.3	2.3–28.2	2.3–28.3	2.3–28.4	2.3–28.3	2.2–28.2
μ (mm^{-1})	0.15	0.15	0.15	0.14	0.14	0.14
Temperature (K)	100 (1)	200 (1)	215 (1)	217 (1)	230 (1)	270 (1)
T_{min}	0.861	0.553	0.331	0.321	0.778	0.797
T_{max}	0.978	0.978	0.979	0.979	0.979	0.979
No. of measured, independent and observed reflections	9480, 2263, 2126	7874, 2456, 2397	8726, 2442, 2299	5924, 889, 800	5804, 923, 859	5918, 940, 820
R_{int}	0.019	0.029	0.026	0.050	0.023	0.023
θ_{max} (°)	28.3	28.3	28.3	28.4	28.3	28.3
Range of h, k, l	$-7 \Rightarrow h \Rightarrow 7$ $-16 \Rightarrow k \Rightarrow 16$ $-11 \Rightarrow l \Rightarrow 11$	$-7 \Rightarrow h \Rightarrow 7$ $-16 \Rightarrow k \Rightarrow 16$ $-11 \Rightarrow l \Rightarrow 11$	$-8 \Rightarrow h \Rightarrow 8$ $-16 \Rightarrow k \Rightarrow 16$ $-11 \Rightarrow l \Rightarrow 11$	$-8 \Rightarrow h \Rightarrow 7$ $-16 \Rightarrow k \Rightarrow 16$ $-11 \Rightarrow l \Rightarrow 11$	$-8 \Rightarrow h \Rightarrow 8$ $-16 \Rightarrow k \Rightarrow 16$ $-11 \Rightarrow l \Rightarrow 11$	$-8 \Rightarrow h \Rightarrow 8$ $-16 \Rightarrow k \Rightarrow 16$ $-11 \Rightarrow l \Rightarrow 11$
$R[F^2 > 2\sigma(F^2)]$, $wR(F^2)$, S	0.032, 0.085, 1.11	0.087, 0.197, 1.31	0.069, 0.194, 1.19	0.061, 0.154, 1.25	0.043, 0.112, 1.14	0.041, 0.116, 1.11
No. of reflections	2263	2456	2442	889	923	940
No. of parameters	120	120	120	82	82	83
H-atom treatment	Mixture of independent and constrained refinement	Mixture of independent and constrained refinement	Mixture of independent and constrained refinement	Only coordinates refined	Only coordinates refined	Only coordinates refined
Weighting scheme	$w = 1/[\sigma^2(F_o^2) + (0.0407P)^2 + 0.142P]$, where $P = (F_o^2 + 2F_c^2)/3$	$w = 1/[\sigma^2(F_o^2) + (0.0377P)^2 + 1.4289P]$, where $P = (F_o^2 + 2F_c^2)/3$	$w = 1/[\sigma^2(F_o^2) + (0.0892P)^2 + 0.5663P]$, where $P = (F_o^2 + 2F_c^2)/3$	$w = 1/[\sigma^2(F_o^2) + (0.0547P)^2 + 0.6287P]$, where $P = (F_o^2 + 2F_c^2)/3$	$w = 1/[\sigma^2(F_o^2) + (0.0527P)^2 + 0.2709P]$, where $P = (F_o^2 + 2F_c^2)/3$	$w = 1/[\sigma^2(F_o^2) + (0.0639P)^2 + 0.1693P]$, where $P = (F_o^2 + 2F_c^2)/3$
$(\Delta/\sigma)_{max}$	0.009	0.004	0.006	<0.0001	<0.0001	<0.0001
$\Delta\rho_{max}$, $\Delta\rho_{min}$ (e Å^{-3})	0.32, −0.30	0.50, −0.58	0.41, −0.43	0.35, −0.28	0.35, −0.20	0.24, −0.29
Extinction method	None	None	None	None	None	*SHELXL*
Extinction coefficient	n/a	n/a	n/a	n/a	n/a	0.040 (7)

Experimental parameters common to all data collections: chemical formula: $C_4H_4N_2O_3{\cdot}2H_2O$; M_r = 164.12; Z = 4; radiation type = Mo $K\alpha$; crystal form and colour: colourless block; crystal size (mm): 0.53 × 0.42 × 0.15; diffractometer: Bruker SMART 1K CCD; data collection method: thin-slice ω scans; absorption correction: multi-scan (based on symmetry-related measurements); criterion for observed reflections: $I > 2\sigma(I)$; refinement on: F^2. Computer programs used: *SMART* (Bruker, 2001), *GEMINI* (Bruker, 2001), *SAINT* (Bruker, 2001), *SHELXTL* (Sheldrick, 2001) and local programs.

the crystal was not removed from the goniometer head between data collections, and a visual examination of the crystal at the end of the experiments showed that it suffered no physical effects (*e.g.* cracking) as a result of the cooling and heating. Ultimately the same crystal stayed attached to the goniometer head for over 2 weeks.

The true crystal temperature was verified by collecting data on a crystal of $CsOH{\cdot}H_2O$ (purchased from Lancaster Synthesis). Caesium hydroxide monohydrate is known to undergo a phase transition from *C*-centred monoclinic to hexagonal at 229 K (Tomaszewski, 1992). This phase transition was observed at 228–229 K and so the crystal temperature as reported by the Cryostream was found to be reliable. After each temperature change the crystal of barbituric acid dihydrate was allowed to stabilize at the new temperature for around 30 min before starting the data collection.

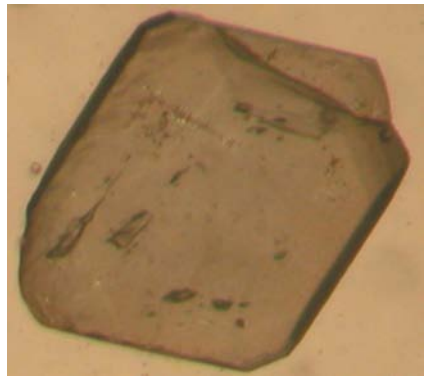

Figure 1
The crystal after two weeks on the diffractometer. The apparent defect at the top right is a ridge in the crystal and not a crack. Other apparent defects on the face of the crystal are air bubbles in the oil used to coat and store the crystal.

Table 2
Summary of results for refinements at each temperature.

Temperature (K)	Space group	Data to $2\theta = 52^\circ$ R $[F_o^2 > 4\sigma(F_o^2)]$	Data to $2\theta = 52^\circ$ wR (all F^2)	Data to $2\theta = 50^\circ$ R $[F_o^2 > 4\sigma(F_o^2)]$	Data to $2\theta = 50^\circ$ wR (all F^2)
100	$P2_1/n$	0.0319	0.0827	0.0291	0.0927
150	$P2_1/n$	0.0505	0.1309	0.0384	0.1098
170	$P2_1/n$	0.0397	0.1027	0.0341	0.1000
190	$P2_1/n$	0.0374	0.1004	0.0343	0.1124
200	$P2_1/n$	0.0869	0.1967	0.0618	0.1540
210	$P2_1/n$	0.0664	0.1496	0.0462	0.1176
215	$P2_1/n$	0.0690	0.1919	0.0522	0.1591
216	$P2_1/n$	0.0684	0.1806	0.0508	0.1477
217	*Pmnb*	0.0611	0.1504	0.0469	0.1277
218	*Pmnb*	0.0539	0.1337	0.0425	0.1156
219	*Pmnb*	0.0664	0.1597	0.0479	0.1264
220	*Pmnb*	0.0453	0.1198	0.0391	0.1083
230	*Pmnb*	0.0429	0.1095	0.0332	0.0914
270	*Pmnb*	0.0415	0.1239	0.0323	0.0886

2.4. Data processing

For each collection the data were processed both as monoclinic and as orthorhombic, regardless of the symmetry implied by the data. This approach proved especially important for those data sets collected around the transition temperature. For example, those data sets which were clearly monoclinic were also processed as orthorhombic, with the β angle constrained in cell refinement after integration and the space group set as *Pmnb*. We chose this unconventional setting of *Pnma* so that the unit-cell axes matched those of the monoclinic space group $P2_1/n$, thus allowing for detailed comparison of the two structures. Similarly the orthorhombic data sets were integrated as monoclinic with no constraints on the β angle and the space group $P2_1/n$ selected. By treating each data set in this way and comparing the final monoclinic and orthorhombic refinement results it was, in most cases, obvious which was correct and which was incorrect.

Starting with the 150 K collection the programs *GEMINI* and *SMART* (Bruker, 2001) were used to determine and refine both components of the twin. *SAINT* (Bruker, 2001) was then used to integrate the data and *TWINABS* (Sheldrick, 2002) was used to correct for absorption and other effects and to write two corrected data files for structure solution and refinement. The *SHELXTL* suite of programs was used for space group determination, structure solution and refinement (Sheldrick, 2001). Having refined the structure as non-merohedrally twinned monoclinic to a satisfactory conclusion the data processing was repeated as described above with orthorhombic constraints. We used *SADABS* (Sheldrick, 2003) and not *TWINABS* for absorption correction of the (untwinned) orthorhombic data sets. Molecular diagrams and other graphics were produced using *DIAMOND* (Brandenburg & Putz, 2004) and *MERCURY* (Version 1.3; Bruno *et al.*, 2002).

This approach was followed for all other data collections, and the non-H atomic coordinates from the 150 K collection were used as starting parameters for structure refinement at all other temperatures. This procedure ensured that factors such as unit-cell origin, atomic coordinates and atomic labels were consistent throughout. Appropriate adjustments were made to the coordinates of the structures in *Pmnb* to constrain the atoms to lie on the mirror plane in accordance with the space-group symmetry. Anomalies in some of the transmission factor ranges are discussed below.

3. Results and discussion

A summary of the refinement results for each data collection is presented as Table 2. Examination of the results at each temperature shows that it is possible to classify each one as definitely monoclinic, definitely orthorhombic or 'transitional', where it is not immediately obvious which is the most appropriate space group, and in some cases both crystal systems seem appropriate. The *ADDSYM* function of *PLATON* (Spek, 2003) was very useful in the detection of additional symmetry in the monoclinic structures.

3.1. Diffraction patterns

Examination of the diffraction pattern is the most reliable way of determining the correct crystal system of a structure. As a simple example, Fig. 2 shows three screenshots of a frame recorded at 100, 215 and 230 K with the crystal in the same orientation. On each frame two pairs of reflections have been highlighted. They share common h and k indices but differ in the value of l (as indicated on the 230 K frame). One reflection of each pair belongs to one component of the twin and the other reflection belongs to the second component of the twin. The two components are related by a 180° rotation about the c axis. At 100 K, a monoclinic temperature, the reflections are well separated and the program *GEMINI* could easily index both twin components. As the temperature increases the reflections begin to move closer together and at 215 K, a transitional temperature, they are starting to merge. Indexing the diffraction pattern is now not so easy, and both monoclinic and orthorhombic unit cells can be determined. At 230 K pairs of reflections have merged completely, to give discrete reflections with unique indices, and the structure is now orthorhombic.

3.2. Unit-cell parameters

Table 3 gives unit-cell parameters for all experiments. Phase transitions are often accompanied by a significant change in unit-cell dimensions, such as the doubling of an axis. Here there is little change in the size of the unit cell save for a gradual increase in unit-cell volume so that the unit cell at 270 K is around 19 Å^3 larger than that at 100 K. This difference is largely insignificant, given that unit cells measured at or near room temperature are generally larger than those measured at low temperatures.

3.3. Orthorhombic structures

Data collected at 220, 230 and 270 K are classed as definitely orthorhombic. At these temperatures *GEMINI* was unable to determine two separate twin components from the

Table 3
Unit-cell parameters for all data collections.

Temperature (K)	*a*	*b*	*c*	α	β	γ	Volume
100	6.0970 (5)	12.7152 (1)	8.8587 (7)	90	94.051 (1)	90	685.05 (9)
150	6.1130 (8)	12.7149 (2)	8.8564 (1)	90	93.437 (2)	90	687.14 (2)
170	6.1270 (5)	12.7253 (1)	8.8633 (8)	90	93.068 (2)	90	690.06 (1)
190	6.1377 (5)	12.7306 (1)	8.8641 (8)	90	92.528 (2)	90	691.94 (1)
200	6.1313 (1)	12.7032 (2)	8.8456 (2)	90	92.187 (4)	90	688.45 (2)
210	6.1538 (2)	12.7474 (3)	8.8776 (2)	90	91.627 (4)	90	696.05 (3)
215	6.1580 (9)	12.7515 (2)	8.8963 (1)	90	91.263 (3)	90	698.40 (2)
216	6.1567 (2)	12.7329 (3)	8.8646 (2)	90	91.180 (5)	90	694.77 (3)
217	6.1770 (2)	12.7851 (2)	8.8984 (3)	90	90	90	702.70 (3)
218	6.1626 (2)	12.7574 (4)	8.8763 (1)	90	90	90	697.80 (4)
219	6.1624 (2)	12.7569 (3)	8.8782 (2)	90	90	90	697.94 (3)
220	6.1665 (1)	12.7626 (4)	8.8814 (2)	90	90	90	698.99 (2)
230	6.1739 (4)	12.7594 (9)	8.8831 (6)	90	90	90	699.77 (8)
270	6.2144 (7)	12.7512 (1)	8.8841 (1)	90	90	90	703.99 (1)

diffraction patterns so the possibility that the data were non-merohedrally twinned was discarded. Orthorhombic and pseudo-orthorhombic models both gave similar satisfactory values of *R* when refinement had converged, so we examined the pseudo-orthorhombic models for additional symmetry. The use of *ROTAX* (Cooper *et al.*, 2002) showed that 180° rotations were possible about the [100], [010] and [001] reciprocal and direct lattice directions, and analysis with *ADDSYM* showed an additional mirror plane missing from the model. It was simple to conclude that, at these temperatures, the structures are indeed, as has twice been reported, best described in the higher-symmetry space group *Pmnb* (or *Pnma*) rather than in $P2_1/n$.

Taking the structure at 230 K as an example, a displacement ellipsoid plot and a packing diagram viewed along the *c* axis of (I) are given in Fig. 3. H atoms were all located in a difference map and refined with $U_{iso} = 1.2U_{eq}$(C,N,O); their coordinates were refined freely. All atoms, with the exception of the CH_2 H atoms, lie on the mirror plane (one of the H atoms in the ellipsoid plot is symmetry generated); this fact is neatly shown by the packing diagram. The two water molecules are coplanar with the barbituric acid ring. Molecular dimensions are unexceptional and in agreement with those reported by Al-Karaghouli *et al.* (1977), with the exception of the *X*—H bonds, which are around 0.1–0.2 Å shorter than the previously reported values. This difference is to be expected, since ours is

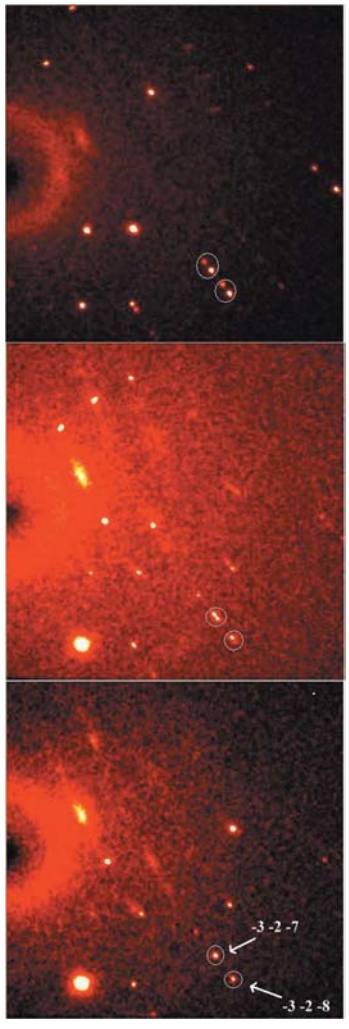

Figure 2
Three frames from data collections at 100 K (top), 215 K (centre) and 230 K (bottom).

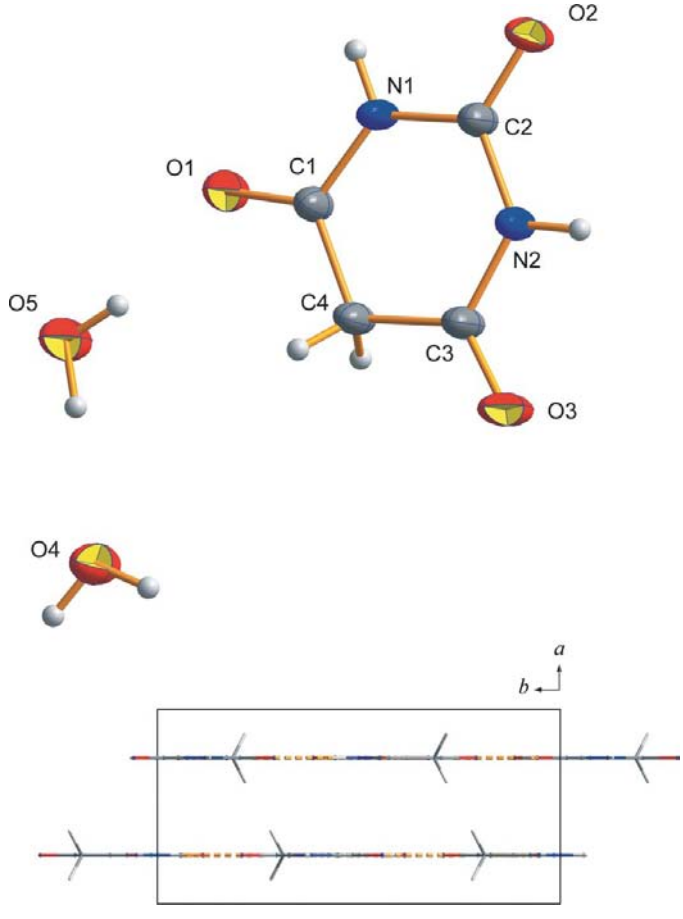

Figure 3
Displacement ellipsoid plot (50% probability) and packing diagram along the *c* axis of the 230 K structure. Hydrogen bonds are indicated in orange.

Table 4
Selected geometric parameters (Å, °) from the monoclinic 100 K structure.

Atom sites	Bond lengths	Atom sites	Bond angles	Atom sites	Torsion angles
N1—C1	1.3643 (13)	O1—C1—C4	121.62 (9)	C2—N1—C1—C4	−4.70 (16)
N1—C2	1.3810 (13)	N1—C1—C4	117.59 (9)	C2—N2—C3—C4	6.22 (17)
N2—C2	1.3728 (13)	O3—C3—C4	123.01 (9)	O1—C1—C4—C3	−172.47 (10)
N2—C3	1.3670 (13)	N2—C3—C4	117.29 (9)	N1—C1—C4—C3	9.09 (15)
C1—C4	1.5034 (14)	C1—C4—C3	115.90 (8)	O3—C3—C4—C1	171.19 (11)
C3—C4	1.5054 (14)			N2—C3—C4—C1	−9.76 (15)

an X-ray diffraction study and we are comparing it with neutron diffraction results.

3.4. Monoclinic structures

Those structures determined at 100, 150, 170 and 190 K are classed as definitely monoclinic with space group $P2_1/n$. In each case the diffraction pattern is non-merohedrally twinned. That the diffraction pattern is twinned as a result of the orthorhombic-to-monoclinic transition is not surprising and is quite common in situations of a material changing from higher to lower symmetry. The two components of the twin are related by a 180° rotation about the c axis, and at low temperatures the extent of the twinning is such that one can clearly see the reflections from both components in the diffraction pattern, as shown in Fig. 2. Attempts to refine these data with orthorhombic models result in refinements with very large R factors. Another curious feature is the change in the magnitude of the β angle with temperature; as shown in Table 3, the β angle approaches 90° as the temperature increases towards the phase transition. All of these structures share another common feature in that the barbituric acid molecule is no longer planar. In this space group there is no imposed mirror symmetry and as a result the Csp^3 (C4) atom, with its tetrahedral rather than trigonal geometry, is seen to deviate from the mean plane of the rest of the molecule.

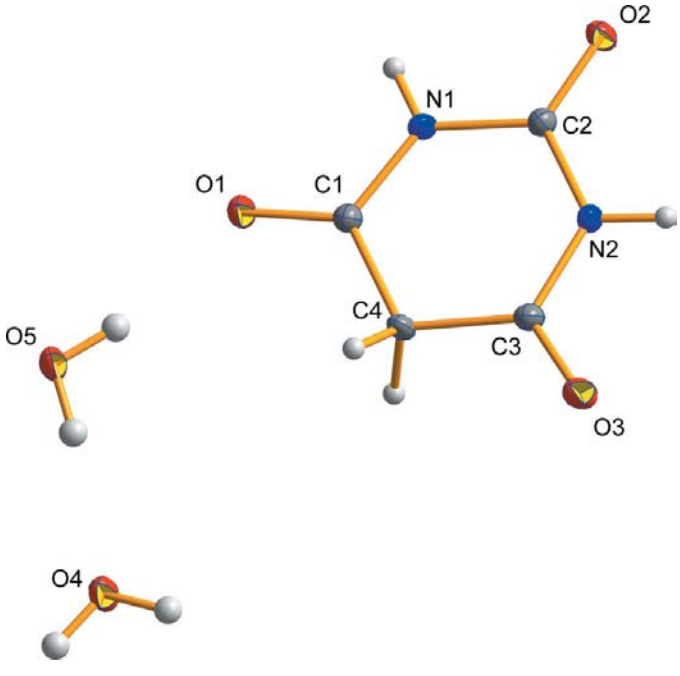

Figure 4
Displacement ellipsoid plot (50% probability) of the 100 K structure.

Fig. 4 shows a displacement ellipsoid plot of (I) at 100 K. All H atoms were identified in a difference electron density map and their coordinates were refined, with the exception of the CH_2 H atoms, which were positioned geometrically (C—H = 0.99 Å) and constrained as riding during refinement. All H atoms were refined with $U_{iso} = 1.2U_{eq}$(O,N,C). Molecular dimensions, listed in Table 4, are unexceptional and, with the exception of the torsion angles, are more or less the same as those determined at 230 K. Fig. 5 shows an overlay of the monoclinic structure at 100 K (red) and the orthorhombic structure at 230 K (black), produced by plotting the mean plane (r.m.s. deviation 0.0288 Å) of atoms C1, O1, N1, C2, O2, C2, N2, C3 and O3 of the monoclinic 100 K structure against the planar ring of the orthorhombic 230 K structure. The out-of-plane displacement of the C4 atom can be clearly seen. This is not an unprecedented observation; the structure of unsolvated barbituric acid shows a similar puckering in the ring (Bolton, 1963; Lewis *et al.*, 2004). By using the *CALCALL* function of *PLATON* we determined the Cremer–Pople ring puckering parameter Q at 100 K to be 0.0787 Å. This is a very small value but does indicate that at 100 K the ring is distorted to a measurable degree in the envelope conformation. At higher temperatures the ring puckering is less significant and *CALCALL* does not report it. This small, but significant, conformational flexibility of the barbituric acid molecule has proved to be a major obstacle in polymorph prediction (Lewis *et al.*, 2004).

In addition to the ring puckering, the two water molecules are no longer coplanar with the barbituric acid ring. This is a more significant change from the orthorhombic structure and, as a consequence, the molecular packing shows some obvious differences. Fig. 6 shows a packing diagram of the structure at 100 K, viewed along the c axis. The hydrogen-bonding motifs in both the orthorhombic and the monoclinic structures are identical but here, because the water molecules are no longer coplanar with the barbituric acid molecules, some adjustment in the packing is necessary to preserve the hydrogen-bonding arrangement. Thus, instead of observing perfectly planar sheets of hydrogen-bonded water and barbituric acid molecules, we see sheets that are now rippled in appearance. Hydrogen-bonding parameters are given in Table 5.

3.5. Transitional structures

The structures refined from data collected between 200 and 219 K are classed as 'transitional'; that is to say, aspects of the data and the refinement imply that the structure is undergoing change of some sort. Table 6 gives details of the final refinement outcomes for both space groups and shows also the

Table 5
Hydrogen-bonding geometry in the monoclinic 100 K structure.

	D—H	H···*A*	*D*···*A*	*D*—H···*A*
O4—H1O···O2^{i}	0.819 (17)	1.969 (17)	2.7583 (11)	161.9 (16)
O4—H2O···O1^{ii}	0.822 (17)	2.034 (17)	2.8508 (11)	172.4 (15)
O5—H3O···O4	0.821 (18)	1.931 (19)	2.7463 (12)	171.7 (17)
O5—H4O···O1	0.828 (17)	1.967 (18)	2.7819 (12)	167.9 (16)
N1—H1N···O3^{iii}	0.823 (15)	1.986 (16)	2.8084 (12)	177.2 (14)
N2—H2N···O5^{iv}	0.874 (15)	1.861 (15)	2.7277 (12)	171.2 (14)

Symmetry codes: (i) $\frac{1}{2}-x,\frac{1}{2}+y,\frac{3}{2}-z$; (ii) $\frac{1}{2}-x,\frac{1}{2}+y,\frac{1}{2}-z$; (iii) $\frac{1}{2}-x,-\frac{1}{2}+y,\frac{3}{2}-z$; (iv) $x, y, 1+z$.

unconstrained β angle as determined in the monoclinic models. At these temperatures the choice of monoclinic *versus* orthorhombic was not immediately obvious, and several different approaches to each data set were tried in order to determine which cell setting and space group best described the data.

As can be seen from the refinement results presented in Tables 2 and 6, data quality at these temperatures was much poorer than those at lower or higher temperatures. In particular, the data above $2\theta = 50^{\circ}$ were much weaker than previously observed, and removal of these data from the refinement led to a marked improvement in the quality of *R* and *wR*. High-angle data quality usually depends on factors such as crystal size and quality, scattering power of the atoms, disorder within the structure, and temperature of data collection. In this study the same crystal was used throughout and the structure is rigid with little scope for disorder, leaving just the effect of increasing temperature as a possible cause of weaker high-angle data. It is true that the lower the crystal temperature, the higher the diffracted X-ray intensities are, and so the more distinguishable from the background are the reflections. However, this fact would not account for such a marked decrease in the data quality from 190 to 200 K. Usually in such a case one would be justified in omitting these poor data from the least-squares calculations. However, this approach would not be appropriate in this case. That the high-angle data at transitional temperatures are poor in comparison to other collections is a significant observation in this study, and it is for this reason that the resolution of the refinement and structure reporting were not restricted to $2\theta_{max} = 50^{\circ}$.

Another significant observation is the difference between the minimum and maximum transmission factors resulting from the *TWINABS*/*SADABS* scaling, as presented in Table 1. The differences between T_{min} and T_{max} at 100, 230 and 270 K are reasonable; however, those reported at 200, 215 and 217 K are not. *TWINABS* and *SADABS* correct for absorption by comparing the intensities of supposedly equivalent (by symmetry) or repeated (as a result of collecting redundant data) reflections. Given that the same crystal was used for all experiments, the large range of transmission at these intermediate temperatures cannot be connected to the shape or size of the crystal. Each data set was collected using an identical strategy, ruling out the possibility of variation due to changes in experimental settings. The wide variations in the putative absorption corrections must be a partial compensation for the poor quality of data from an intermediate structural state by the frame-scaling procedure in these multi-scan correction methods. We do not believe the variations are due to any hysteresis effect of structural change lagging behind temperature change, since the phase transition is not a large one, and the crystal was held at each new temperature for at least 30 min before data collection began. However, it should be noted that the temperature interval between these data sets is of the same order as the uncertainty in the temperature itself. If the phase transition is one that takes place gradually over a range of several degrees in temperature then some minor variation in the structure, and hence in the diffraction pattern, during each data collection is likely. These intermediate structures should each be regarded as an average

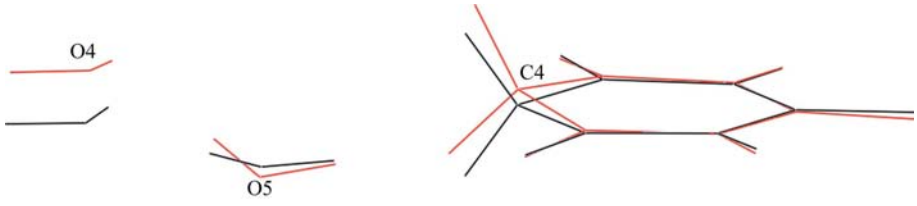

Figure 5
Overlay of the 100 K structure (red) and 230 K structure (black) showing the out-of-plane displacement of the C4 atom and the two water molecules.

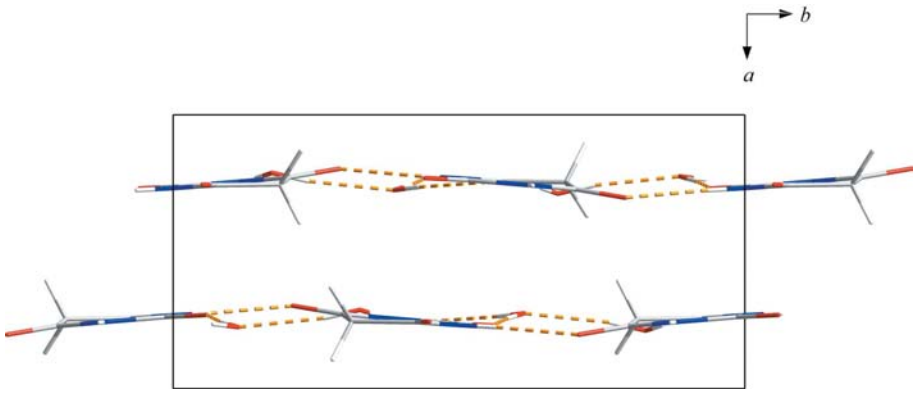

Figure 6
Packing diagram along the *c* axis of the 100 K structure. Hydrogen bonds are marked in orange.

Table 6
Comparison of refinement details for transitional structures.

Temperature	β angle	R for $2\theta < 52^\circ$		R for $2\theta < 50^\circ$		Mirror plane detected by
(K)	(unconstrained)	$P2_1/n$	*Pnmb*	$P2_1/n$	*Pnmb*	*ADDSYM* (in $P2_1/n$?
200	92.187 (4)	0.0869	0.1020	0.0618	0.0669	No
210	91.627 (4)	0.0664	0.093	0.0462	0.0789	No
215	91.263 (3)	0.0690	0.0865	0.0522	0.0632	No
216	91.180 (5)	0.0684	0.0743	0.0508	0.0546	No
217	90.952 (4)	0.0741	0.0611	0.0596	0.0469	Yes
218	90.139 (4)	0.0670	0.0539	0.0500	0.0425	Yes
219	90.071 (3)	0.0764	0.0664	0.0571	0.0479	Yes
220	90.149 (3)	0.0493	0.0453	0.0428	0.0391	Yes

structure over a small temperature range, and the range of transmission factors probably reflects this, together with the generally poorer refinement results compared with those at higher and lower temperatures where a single phase is present.

3.5.1. Structures at 200, 210, 215 and 216 K. After much experimentation, several unit-cell determinations, the creation of many different models and seemingly endless refinement cycles, it was concluded that, at these temperatures, the crystal structures are better described as monoclinic rather than orthorhombic. However, in each case the decision was very close and, if taken based on refinement alone, would have been difficult to determine. To verify that orthorhombic was not a more appropriate description of the data, *ADDSYM* was used to detect missed symmetry and in each case none was detected. The data collected at 215 and 216 K are of particular interest. Examination of the diffraction pattern at 215 K showed pairs of reflections and, although the separation of the reflections was quite small, they are an indicator of twinning. However, at 216 K there are virtually no pairs of reflections; instead they are seen merged and take the form of smeared ellipses rather than separate discrete isotropic spots. Refinement of the orthorhombic model gave a similar result to that of the monoclinic model, and it is possible that there was a combination of both monoclinic and orthorhombic unit cells coexisting in equilibrium at the same time.

3.5.2. Structures at 217, 218 and 219 K. At these temperatures the balance begins to tip towards the orthorhombic crystal system. The first major observation at 217 K is that the non-merohedrally twinned crystal system is no longer an appropriate model for the data. Although *GEMINI* was able to determine two orientation matrices, refinement of the structure was poor, giving very high values of R and wR (0.133 and 0.278, respectively). The refined twin fraction had a very high uncertainty, thus making the parameter (and therefore the twinning) meaningless. As a result the non-merohedrally twinned monoclinic model was quickly discarded. A pure (*i.e.* untwinned) monoclinic model was tried, giving a slightly better result; however, both *ADDSYM* and *ROTAX* suggested that this model was no longer appropriate. Although the unconstrained β angle is still almost a degree away from 90°, at 217 K the orthorhombic model gives the most satisfactory refinement result and we can say that the orthorhombic model is, on balance, the better way to describe the data. At 218 and 219 K the refinement results for the orthorhombic system become increasingly more favourable, and we now are more-or-less able to disregard the monoclinic crystal system as a reliable way of describing the structure; rather than being merely 'better described' as orthorhombic they are now clearly orthorhombic – a subtle but important difference.

4. Conclusions

The two previously reported crystal structures of barbituric acid dihydrate in space group *Pnma* only hold true at temperatures above 220 K. Below 200 K the crystal structure is better described as non-merohedrally twinned monoclinic in space group $P2_1/n$, and between 200 and 220 K the crystal structure undergoes a phase transition from monoclinic to orthorhombic. The phase transition is not particularly sharp; whilst the point at which the majority of the diffraction pattern changes from monoclinic to orthorhombic is probably around 216–217 K, the full transition appears to take place over a rather wider temperature range. The transition is reversible and the crystal suffers no physical effects as a result of either the temperatures used or the transition itself.

In the monoclinic structure the magnitude of the β angle is seen to vary with temperature. The angle approaches 90° as the temperature approaches the phase transition. There are no other significant changes in unit-cell dimensions and the observed increase in unit-cell volume is insignificant.

The structural differences in changing from the orthorhombic to monoclinic phase are most clearly seen by looking at the displacement of the Csp^3 atom of the barbituric acid ring and the significant movement of the two water molecules away from coplanarity with the barbituric acid, as presented in Fig. 5. The orthorhombic phase features all atoms (with the exception of the CH_2 H atoms) lying on the mirror plane imposed by the space group, although in the monoclinic phase this is no longer a symmetry requirement and the molecules have the freedom to distort and shift. The hydrogen-bonding motif of both the orthorhombic and monoclinic phases is the same; however, the physical arrangement of the molecules is different, and this difference is best seen by viewing and comparing *c*-axis projections of the orthorhombic and monoclinic phases.

We thank Dr Neil Brooks and Dr Ross Harrington, Newcastle University, for advice related to twinning and for experimental assistance, the EPSRC for financial support, and Professor Sally Price, University College London, for helpful discussions and pre-publication results relating to polymorph prediction for barbituric acid.

References

Al-Karaghouli, A. R., Abdul-Wahab, B., Ajaj, E. & Al-Asaff, S. (1977). *Acta Cryst.* B**33**, 1655–1660.
American Chemical Society (2004). SciFinder Scholar Version 2004.2. http://www.cas.org/SCIFINDER/SCHOLAR/.
Brandenburg, K & Putz, H. (2004). *DIAMOND*. Version 3. University of Bonn, Germany.
Bolton, W. (1963). *Acta Cryst.* **16**, 166–173.
Bruker (2001). *GEMINI*, *SMART* and *SAINT*. Bruker AXS Inc., Madison, Wisconsin, USA.
Bruno, I. J., Cole, J. C., Edgington, P. R., Kessler, M., Macrae, C. F., McCabe, P., Pearson, J. & Taylor, R. (2002). *Acta Cryst.* B**58**, 389–397.
Caillet, J. & Claverie, P. (1980). *Acta Cryst.* B**36**, 2642–2645.
Cleverley, B. & Williams, P. P. (1959). *Tetrahedron*, **7**, 277–288.
Cooper, R. I., Gould, R. O., Parsons, S. & Watkin, D. J. (2002). *J. Appl. Cryst.* **35**, 168–174.
Cosier, J. & Glazer, A. M. (1986). *J. Appl. Cryst.* **19**, 105–107.
Craven, B. M., Fox, R. O. & Weber, H.-P. (1982). *Acta Cryst.* B**38**, 1942–1952.
Craven, B. M. & Vizzini, E. M. (1969). *Acta Cryst.* B**25**, 1993–2009.
Craven, B. M. & Vizzini, E. M. (1971). *Acta Cryst.* B**27**, 1917–1924.
Craven, B. M., Vizzini, E. M. & Rodrigues, M. M. (1969). *Acta Cryst.* B**25**, 1978–1993.
Jeffrey, G. A., Ghose, S. & Warwicker, J. O. (1961). *Acta Cryst.* **14**, 881–887.
Lewis, T. C., Tocher, D. A. & Price, S. L. (2004). *Cryst. Growth Des.* **4**, 979–987.
Lewis, T. C., Tocher, D. A. & Price, S. L. (2005). *Cryst. Growth Des.* **5**, 983–993.
McMullan, R. K., Craven, B. M. & Fox, R. O. (1978). *Acta Cryst.* B**34**, 3719–3722.
Nichol, G. S. & Clegg, W. (2005*a*). *Acta Cryst.* C**61**, o297–o299.
Nichol, G. S. & Clegg, W. (2005*b*). *Acta Cryst.* E**61**, o1004–o1006.
Pandey, D. (2005). *Acta Cryst.* A**61**, 1–2.
Platteau, C., Lefebvre, J., Hemon, S., Baehtz, C., Danede, F. & Prevost, D. (2005). *Acta Cryst.* B**61**, 80–88.
Sambyal, V. S., Goswami, K. N. & Kahjuria, R. K. (1995). *Cryst. Res. Technol.* **30**, 817–823.
Sheldrick, G. M. (2001). *SHELXTL*. Version 6. Bruker AXS Inc., Madison, Wisconsin, USA.
Sheldrick, G. M. (2002). *TWINABS*. University of Göttingen, Germany.
Sheldrick, G. M. (2003). *SADABS*. University of Göttingen, Germany.
Spek, A. L. (2003). *J. Appl. Cryst.* **36**, 7–13.
Tomaszewski, P. (1992). *Phase Transit.* **38**, 127–220.
Williams, P. P. (1973). *Acta Cryst.* B**29**, 1572–1579.
Williams, P. P. (1974). *Acta Cryst.* B**30**, 12–17.